ACTIVE VIBRATION CONTROL OF TWO-BEAM STRUCTURES

Chen Tao(陈涛), *Wang Ligang*(王立刚), *Feng Guofeng*(冯国锋)

(College of Science, Harbin Engineering University, Harbin, 150001, P. R. China)

Abstract: The wave propagation approach is presented to research the active vibration control of two-beam structures. Considering the continuity of the generalized displacement and the equilibrium of the generalized force at the discontinuity, the wave reflection and transmission coefficients are calculated. Wave control is applied somewhere upstream or downstream to two-beam structures. Vibrations of two coupled beams per unit disturbance are investigated. The results show that wave control is efficient, and the influence of the thickness ratio of two-beam structures on control location is discussed.

Key words: two-beam structures; vibration control; reflection coefficients; transmission coefficients

CLC number: O32 **Document code**: A **Article ID**: 1005-1120(2013)02-00193-09

INTRODUCTION

Two-beam structures are commonly used as elements in the construction of many practical engineering structures such as spacecraft and large space structures. All these structures have flexible extensions which are made as light and slender as possible. Such slender elements lack the necessary damping properties of being able to function effectively under dynamic loads. In order to damp out excessive vibrations and improve the performance of structures, conventional approaches of additional passive damping treatments are not often implemented on these systems because of weights or other constraints. Therefore there has been an increasing interest in active vibration control[1-4]. In active vibration control, desirable performance characteristics are achieved through the application of control forces to a structure.

Vibrations can be described in a number of ways, with the most common descriptions in terms of modes and wave motion. In modal active vibration control, the aim is to control the characteristics of the modes of vibration, i. e., their damping factors, natural frequencies or mode shapes. Modal control aims to control the global behavior of the structure, whereas wave control aims to control the flow of vibration energy through the structure. Wave designs are based on the local properties of the structure, and are inherently much less sensitive to system properties and more robust than global models of structures[5-6]. In a continuous structure, vibrations can alternatively be regarded as the superposition of waves traveling through the structure. These waves are reflected and transmitted at the structural discontinuities. Active wave control aims to control the distribution of energy in the structure by either reducing the transmission of waves from one part of the structure to another or absorbing the energy carried by the waves. Here the disturbance is detected, and a control force is used somewhere upstream or downstream to absorb the energy associated with the propagating wave.

Physical modes of flexural wave propagation in beam or plate are developed in order to implement wave control. Gardonio and Elliott controlled a one-dimensional structure with a scattering termination by means of active control of

Foundation items: Supported by the National Natural Science Foundation of China(11102047, 11002037); the Special Funds of Central Colleges Basic Scientific Research Operating Expenses(HEUCF20111139); the Fundamental Research Foundation of Harbin Engineering University(002110260746).

Received date: 2011-07-26; **revision received date**: 2011-09-07

Corresponding author: Chen Tao, Lecturer, E-mail: chen_tao1204@163.com.

waves[7]. Brennan described an analytical and experimental investigation into the use of a tunable vibration neutralizer to control the transmission of flexural propagating waves on an infinite beam[8]. Mei, et al studied hybrid wave/mode active vibration control of an Euler-Bernoulli beam[5]. Carvalho and Zindeluk modeled and tackled active control of waves in a Timoshenko beam[9]. Halkyard and Mace analyzed adaptive control of flexural vibration in a beam using wave amplitudes[10]. EL-Khatib, et al concerned with the control of flexural waves in a beam using a tuned vibration absorber[11]. Hu, et al studied vibration control of Timoshenko beam based on hybrid wave/mode method, and compared wave control with modal control[12]. Chen, et al investigated wave control of a cantilevered Mindlin-type plate[6]. Some authors, like Mace and Mead, dedicated their efforts to the wave reflection mechanism[13-14].

In previous investigations, wave control only has been used to control the wave motion in a beam or plate[6-12]. Less frequently, the wave control of two-beam structures has been investigated. Although Svensson, et al theoretically studied the wave scattering and the active modification of wave scattering at structural junctions[15], wave control has not been investigated. In the present work, a cantilever structure is modeled as two-beam structures. Wave-control approach is applied to the structures. In the two-beam structures, the incident propagating wave is reflected and transmitted at the beam junction and control location. Proportional-plus-derivative (PD) feedback wave control is implemented.

This paper presents a theoretical investigation using active control to attenuate the responses associated with two-beam structures. Based on the substructure synthesis method and Hamilton theory, motion equations of the structures are given in terms of the modal coordinates. And wave-control approach is used to absorb vibration energy. In particular, if the beam material is the same on both sides of the beam junction, wave reflection and transmission coefficients at control location are determined by the thickness ratio of the structures. At last, numerical examples are given, and numerical results show the influences of the thickness ratio of two-beam structures on wave control.

1 MOTION EQUATIONS OF COUPLED BEAM STRUCTURE

The general form of the structures considered in this paper is illustrated in Fig. 1. Two uniform beams are joined rigidly along a common edge. Using the substructure synthesis method, a cantilever beam and a free-free beam are coupled, as shown in Fig. 2.

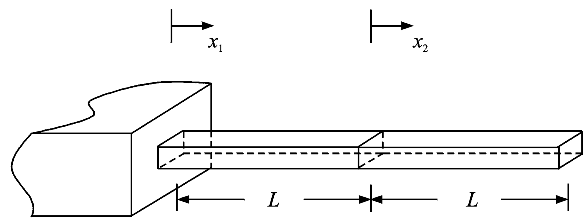

Fig. 1 Cantilever structure of coupled beam

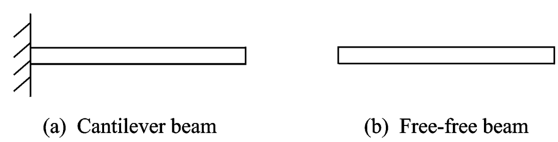

Fig. 2 Cantilever and free-free beams

In the absence of damping, the motion equation of single uniform Euler-Bernoulli beam with constant cross-section may be written in the form

$$(EI)_i \frac{\partial^4 w(x_i,t)}{\partial x_i^{\,4}} + (\rho A)_i \frac{\partial^2 w(x_i,t)}{\partial t^2} = f(x_i,t) \tag{1}$$

where $w(x_1,t)$ and $w(x_2,t)$ are the transversal deflection of the first beam and the second beam, respectively, $f(x_1,t)$ and $f(x_2,t)$ the external disturbance of the first beam and the second beam, respectively, E denotes the Young's modulus, I the area moment of inertia, ρ the density, A the cross-sectional area.

The bending moment M and shear force Q transmitted through an arbitrary section of the beam may be expressed as

$$M = -(EI)_i \frac{\partial^2 w(x_i,t)}{\partial x_i^{\,2}},\ Q = -(EI)_i \frac{\partial^3 w(x_i,t)}{\partial x_i^{\,3}} \tag{2}$$

Using assumed mode method, the displacement of the beam 1 and beam 2 can be discretized as

$$w(x_1,t)=\boldsymbol{\Phi}(x_1)\boldsymbol{q}(t),\ w(x_2,t)=\boldsymbol{\Psi}(x_2)\boldsymbol{p}(t) \tag{3}$$

where $\boldsymbol{\Phi}(x_1)$ and $\boldsymbol{\Psi}(x_2)$ represent the mode functions of transverse vibrations of beam 1 and beam 2, respectively, $\boldsymbol{q}(t)$ and $\boldsymbol{p}(t)$ the modal coordinates of transverse vibrations of beam 1 and beam 2, respectively. The quantities are given by

$$\boldsymbol{\Phi}(x_1)=[\varphi_1(x_1)\quad \varphi_2(x_1)\quad \cdots\quad \varphi_n(x_1)]$$
$$\boldsymbol{q}(t)=[q_1(t)\quad q_2(t)\quad \cdots\quad q_n(t)]^{\mathrm{T}} \tag{4}$$
$$\boldsymbol{\Psi}(x_2)=[\psi_1(x_2)\quad \psi_2(x_2)\quad \cdots\quad \psi_m(x_2)]$$
$$\boldsymbol{p}(t)=[p_1(t)\quad p_2(t)\quad \cdots\quad p_m(t)]^{\mathrm{T}} \tag{5}$$

The kinetic energy of the beam 1 can be expressed as

$$T_1=\frac{1}{2}\int_0^L(\rho A)_1\left[\frac{\partial w(x_1,t)}{\partial t}\right]^2\mathrm{d}x_1=\frac{1}{2}\dot{\boldsymbol{q}}^{\mathrm{T}}\boldsymbol{M}_1\dot{\boldsymbol{q}} \tag{6}$$

where $\boldsymbol{M}_1=\int_0^L(\rho A)_1\boldsymbol{\Phi}^{\mathrm{T}}(x_1)\boldsymbol{\Phi}(x_1)\mathrm{d}x_1$, $(\rho A)_1$ is the mass per unit length of the beam 1, $\dot{\boldsymbol{q}}$ the first derivative with respect to t, and L the length of the beam 1 and beam 2. Here, the mode shapes are assumed to be mass-normalized such that

$$\int_0^L(\rho A)_1\varphi_i(x_1)\varphi_j(x_1)\mathrm{d}x_1=\delta_{ij}\quad i,j=1,2,\cdots \tag{7}$$

The potential energy of the beam 1 can be written as

$$V_1=\frac{1}{2}\int_0^L(EI)_1\left[\frac{\partial^2 w(x_1,t)}{\partial x_1^2}\right]^2\mathrm{d}x_1=\frac{1}{2}\boldsymbol{q}^{\mathrm{T}}\boldsymbol{K}_1\boldsymbol{q} \tag{8}$$

where $\boldsymbol{K}_1=\int_0^L(EI)_1\boldsymbol{\Phi}''^{\mathrm{T}}(x_1)\boldsymbol{\Phi}''(x_1)\mathrm{d}x_1$, $(EI)_1$ is the flexural rigidity of the beam 2, and $\boldsymbol{\Phi}''(x_1)$ the second partial derivatives with respect to x_1.

The kinetic energy of the beam 2 is given by

$$T_2=\frac{1}{2}\int_0^L(\rho A)_2\left[\frac{\partial(w(x_1=L,t)+w(x_2,t))}{\partial t}\right]^2\mathrm{d}x_2=\frac{1}{2}\dot{\boldsymbol{p}}^{\mathrm{T}}\boldsymbol{M}_2\dot{\boldsymbol{p}}+\dot{\boldsymbol{q}}^{\mathrm{T}}\boldsymbol{M}_3\dot{\boldsymbol{p}} \tag{9}$$

where $\boldsymbol{M}_2=\int_0^L(\rho A)_2\boldsymbol{\Psi}^{\mathrm{T}}(x_2)\boldsymbol{\Psi}(x_2)\mathrm{d}x_2$, $\boldsymbol{M}_3=\int_0^L(\rho A)_2\boldsymbol{\Phi}^{\mathrm{T}}(L)\boldsymbol{\Psi}(x_2)\mathrm{d}x_2$, and $(\rho A)_2$ is the mass per unit length of the beam 2. Here, the mode shapes are assumed to be mass-normalized such that

$$\int_0^L(\rho A)_2\psi_i(x_2)\psi_j(x_2)\mathrm{d}x_2=\delta_{ij}\quad i,j=1,2,\cdots \tag{10}$$

The potential energy of the beam 2 is expressed as

$$V_2=\frac{1}{2}\int_0^L(EI)_2\left[\frac{\partial^2 w(x_2,t)}{\partial x_2^2}\right]^2\mathrm{d}x_2=\frac{1}{2}\boldsymbol{p}^{\mathrm{T}}\boldsymbol{K}_2\boldsymbol{p} \tag{11}$$

where $\boldsymbol{K}_2=\int_0^L(EI)_2\boldsymbol{\Psi}''^{\mathrm{T}}(x_2)\boldsymbol{\Psi}''(x_2)\mathrm{d}x_2$, and $(EI)_2$ is the flexural rigidity of the beam 2.

Therefore, the kinetic energy of two-beam structures can be written as

$$T_t=T_1+T_2=\frac{1}{2}[\dot{\boldsymbol{q}}^{\mathrm{T}}\quad \dot{\boldsymbol{p}}^{\mathrm{T}}]\begin{bmatrix}\boldsymbol{M}_1 & \boldsymbol{M}_3\\ \boldsymbol{M}_3 & \boldsymbol{M}_2\end{bmatrix}\begin{bmatrix}\dot{\boldsymbol{q}}\\ \dot{\boldsymbol{p}}\end{bmatrix} \tag{12}$$

The potential energy of the structures is expressed as

$$V=V_1+V_2=\frac{1}{2}[\boldsymbol{q}^{\mathrm{T}}\quad \boldsymbol{p}^{\mathrm{T}}]\begin{bmatrix}\boldsymbol{K}_1 & \boldsymbol{0}\\ \boldsymbol{0} & \boldsymbol{K}_2\end{bmatrix}\begin{bmatrix}\boldsymbol{q}\\ \boldsymbol{p}\end{bmatrix} \tag{13}$$

Substructure synthesis is a method whereby a structure is regarded as an assemblage of substructures, each of which is modeled separately and made to act as a single structure by imposing certain geometric compatibility at boundaries between two adjacent substructures[16]. Therefore, using the substructure synthesis method, the coupled structure is regarded as a cantilever beam and a free-free beam, and applying continuity and equilibrium of the beam junction, dependent modal coordinates $[\boldsymbol{q}^{\mathrm{T}}\ \boldsymbol{p}^{\mathrm{T}}]$ of substructures can be transformed the independent modal coordinates of the coupled structure.

Since the displacement and slope are continuous, furthermore, by considering the equilibrium of the beam junction, constraint equations can be written as

$$w(x_1=L,t)=w_2(x_2=0,t)$$
$$\frac{\partial w(x_1=L,t)}{\partial x_1}=\frac{\partial w_2(x_2=0,t)}{\partial x_2} \tag{14}$$
$$(EI)_1\frac{\partial^2 w(x_1=L,t)}{\partial {x_1}^2}=(EI)_2\frac{\partial^2 w(x_2=0,t)}{\partial {x_2}^2}$$

$$(EI)_1 \frac{\partial^3 w(x_1 = L, t)}{\partial x_1{}^3} = (EI)_2 \frac{\partial^3 w(x_2 = 0, t)}{\partial x_2{}^3} \tag{15}$$

From Eqs. (14—15), the following can be obtained.

$$\begin{bmatrix} \boldsymbol{q} \\ \boldsymbol{p} \end{bmatrix} = \begin{bmatrix} \boldsymbol{G} \\ \boldsymbol{I} \end{bmatrix} \boldsymbol{z} \tag{16}$$

where $\boldsymbol{I}$ is the identical matrix, matrix $\boldsymbol{G}$ can be determined by Eqs. (14—15), and $\boldsymbol{z} = [z_1 \quad z_2 \cdots z_t]^{\mathrm{T}}$ represents modal coordinates of transverse vibrations of two-beam structures.

Substituting Eq. (16) into Eqs. (12—13), we have

$$T_t = \frac{1}{2}\dot{\boldsymbol{z}}^{\mathrm{T}} \boldsymbol{M} \dot{\boldsymbol{z}} \quad V = \frac{1}{2}\boldsymbol{z}^{\mathrm{T}} \boldsymbol{K} \boldsymbol{z} \tag{17}$$

where $\boldsymbol{M} = \boldsymbol{B}^{\mathrm{T}} \begin{bmatrix} \boldsymbol{M}_1 & \boldsymbol{M}_3 \\ \boldsymbol{M}_3 & \boldsymbol{M}_2 \end{bmatrix} \boldsymbol{B}$, $\boldsymbol{K} = \boldsymbol{B}^{\mathrm{T}} \begin{bmatrix} \boldsymbol{K}_1 & \boldsymbol{0} \\ \boldsymbol{0} & \boldsymbol{K}_2 \end{bmatrix} \boldsymbol{B}$, and $\boldsymbol{B} = \begin{bmatrix} \boldsymbol{G} \\ \boldsymbol{I} \end{bmatrix}$.

According to the Clapeyron Principle, the work done by the external load can be expressed as

$$W_e = \frac{1}{2} f(x_1, t) w(x_1, t) + \frac{1}{2} f(x_2, t)(w(x_1 = L, t) + w(x_2, t)) = \boldsymbol{F}^{\mathrm{T}}(t) \boldsymbol{B} \boldsymbol{z} \tag{18}$$

where $\boldsymbol{F}^{\mathrm{T}}(t) = [f(x_1, t)\Phi(x_1) + f(x_2, t)\Phi(L) \quad f(x_2, t)\Psi(x_2)]$, $i = 1, 2$.

Using the Hamilton theory $\int_{t_0}^{t_f} (\delta T_t - \delta V + \delta W_e) \mathrm{d}t = 0$, the equations of motion for two-beam structures can be obtained

$$\boldsymbol{M}\ddot{\boldsymbol{z}} + \boldsymbol{K}\boldsymbol{z} = \boldsymbol{B}^{\mathrm{T}} \boldsymbol{F} \tag{19}$$

Obviously, the natural frequencies of the structures can be determined by $\boldsymbol{M}$ and $\boldsymbol{K}$.

2 FEEDBACK WAVE CONTROL

Vibrations can be regarded as the superstition of the waves traveling through the structure. In this paper, collocated force/sensor negative feedback control is assumed to be applied. In the frequency domain, the wave-control force is given by

$$F(\omega) = -H_w(\omega) w(\omega) \tag{20}$$

where $H_w(\omega)$ is frequency-dependent and complex[5]. Note that the amplitudes of any incident near-field waves are neglected.

A propagating wave is incident on the discontinuity and gives rise to reflected and transmitted waves. In order to determin $H_w(\omega)$, the wave reflection and transmission coefficients at point discontinuities are needed to be calculated.

2.1 Wave transmission and reflection at beam junction

If a concentrated harmonic load is applied, at any point, to the beam, four free flexural waves will emanate from this point.

$$w(x_i) = A_{i1}\exp(-\mathrm{i}k_i x_i) + A_{i2}\exp(\mathrm{i}k_i x_i) + A_{i3}\exp(-k_i x_i) + A_{i4}\exp(k_i x_i) \tag{21}$$

where $k_i = \sqrt[4]{(\rho A)_i \omega^2/(EI)_i}$ $(i = 1, 2)$ are the wavenumbers of elastic wave, $\exp(\mathrm{i}k_i x_i)$ and $\exp(-\mathrm{i}k_i x_i)$ the propagating and energy-carrying waves, whereas $\exp(-k_i x_i)$ and $\exp(k_i x_i)$ the near-field waves carrying no energy, A_{ij} $(j = 1, 2, 3, 4)$ satisfying the boundary condition are the mode coefficients. The aim of the wave control is to absorb the energy associated with the propagating waves.

Let two beams differed by wave-number and bending stiffness be joined at $x_3 = 0$. A positive-propagating wave is incident on the beam junction and gives rise to reflected and transmitted propagating and near-field waves, as shown in Fig. 3.

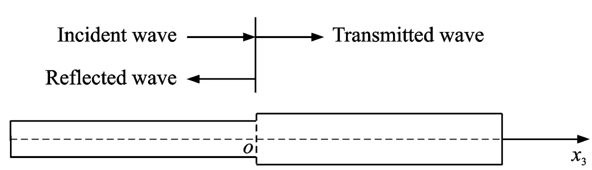

Fig. 3 Reflection and transmission of waves at beam junction

The displacement of the beam $w_-(x_3)$ and $w_+(x_3)$ in the regions $x_3 \leqslant 0$ and $x_3 \geqslant 0$ are given by

$$w_-(x_3) = a^+\exp(-\mathrm{i}k_1 x_3) + a^-\exp(\mathrm{i}k_1 x_3) + a_{\mathrm{N}}^-\exp(k_1 x_3) \tag{22a}$$

$$w_+(x_3) = b^+\exp(-\mathrm{i}k_2 x_3) + b_{\mathrm{N}}^+\exp(-k_2 x_3) \tag{22b}$$

where the time dependence $\exp(\mathrm{i}\omega t)$ has been suppressed, a^+ denotes the wave amplitude of incident propagating waves, a^- the wave amplitude of reflected propagating waves, a_{N}^- the wave amplitude of reflected near-field waves, b^+ the wave amplitude of transmitted propagating waves, and b_N^+ the wave amplitude of transmitted near-field waves. The subscripts 1 and 2 refer to the incident and transmitted sides of the junction, respectively.

Since the displacement, slope, bending moment and shear force are all continuous at the junction[13], we have

$$w_-(0)=w_+(0) \qquad \psi_-(0)=\psi_+(0) \tag{23a}$$

$$M_-(0)=M_+(0) \qquad Q_+(0)=Q_-(0) \tag{23b}$$

where sign "−" and "+" denote the corresponding mechanical quantity in the regions $x_3\leqslant 0$ and $x_3\geqslant 0$, respectively.

Substituting Eq. (22) into Eq. (23), the reflection and transmission coefficients can be expressed as

$$t_1=4(1+\alpha)(1+\beta)/((1+\alpha)^2(1+\beta)^2-(1+\alpha^2)(1-\beta)^2) \tag{24a}$$

$$r_1=(-4(\alpha^2-1)\beta-2\mathrm{i}\alpha(1-\beta)^2)/((1+\alpha)^2(1+\beta)^2-(1+\alpha^2)(1-\beta)^2) \tag{24b}$$

where $\alpha=k_2/k_1$ and $\beta=(EIK^2)_2/(EIK)_1$ represent the ratios of wave-number and bending wave impedance, t_1 and t_2 the transmission coefficients, and r_1 and r_2 the reflection coefficients.

If the material is the same on both sides of the beam junction, we have

$$\alpha=\sigma^{-1/2}, \quad \beta=\sigma^2 \tag{25}$$

where $\sigma=h_2/h_1$ denotes the thickness ratio of two beams.

For an incident propagating wave, the power carried in a propagating wave is proportional to the square of wave amplitude[6,13]. The reflection efficiency, the ratio of reflected to incident power is given by $E_r(\sigma)=|r_1|^2$, and the power transmitted is given by $E_t=1-E_r(\sigma)=|t_1|^2\sigma^{3/2}$. Therefore the power reflected and transmitted per unit incident power is $E_p(\sigma)=|r_1|^2+|t_1|^2\sigma^{3/2}$. Transmitted energy depends on σ.

2.2 Wave transmission and reflection at control location

The power is mostly transmitted at the beam junction when σ is close to 1. The power is mostly reflected at the beam junction when σ approaches 0. Therefore wave control is used somewhere downstream to absorb energy associated with the transmitted propagating wave of the beam junction when σ is close to 1 as shown in Fig. 4(a). When σ approaches 0, wave control is used somewhere upstream to absorb energy associated with the transmitted propagating wave of beam junction as shown in Fig. 4(b). Transmitted (or reflected) propagating wave of the beam junction is incident on the control location and gives rise to reflected and transmitted propagating and near-field waves.

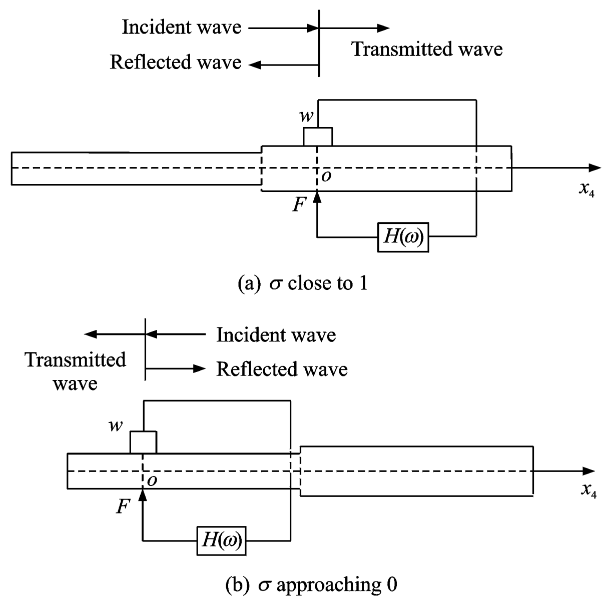

Fig. 4 Schematic diagram of feedback control

At first, consider the first case when σ is close to 1 as shown in Fig. 4(a). Wave control is applied at position $x_4=0$. The displacement of the beam $w^-(x_4)$ and $w^+(x_4)$ in the regions $x_4\leqslant 0$ and $x_4\geqslant 0$ are given by

$$w^-(x_4)=b^+\exp(-\mathrm{i}k_2x_4)+b^-\exp(\mathrm{i}k_2x_4)+b_N^-\exp(k_2x_4) \tag{26a}$$

$$w^+(x_4)=c^+\exp(-\mathrm{i}k_2x_4)+c_N^+\exp(-k_2x_4) \tag{26b}$$

where the time dependence $\exp(\mathrm{i}\omega t)$ has been suppressed.

For the same reason described in Section 2.1, the reflection and transmission coefficients at the control location can be expressed as

$$t_3=1+\frac{\overline{H}\mathrm{i}}{4-(1+\mathrm{i})\overline{H}}, \quad r_3=\frac{\overline{H}\mathrm{i}}{4-(1+\mathrm{i})\overline{H}} \tag{27}$$

where t_3 and t_4 are the transmission coefficients, *and* r_3 and r_4 the reflection coefficients.

In this paper, the controller is designed to absorb vibrational energy by adding optimal damping to the structure. Supposing $\overline{H}(\omega) = (1+\mathrm{i})\omega g$, the power carried in a propagating wave is proportional to the square of the wave amplitude. The performance index of optimal control is to make the dissipated energy at control location the maximum. In other words, the optimal control gain g can be found by assuming that a wave is incident on onside of the control location and then by designing the control gain so as to maximize the absorb incoming energy, namely to minimize $|r_3|^2|t_1|^2\sigma^{3/2}+|t_3|^2|t_1|^2\sigma^{3/2}$.

Therefore the power reflected and transmitted at control location is given by

$$P(g)=(4\sigma^{3/2}(1+\sigma^{-1/2}+\sigma^{3/2}+\sigma^2)^2(4-2g\omega+g^2\omega^2))/((\sigma^{-1/2}+2\sigma+2\sigma^{3/2}+2\sigma^2+\sigma^{7/2})^2(4+g^2\omega^2)) \tag{28}$$

Then the frequency response of the optimal controller is given by

$$\overline{H}_o(\omega)=(1+\mathrm{i})\omega g \tag{29}$$

where $g=2/\omega$.

Next, consider the second case when the power is mostly reflected at the beam junction (σ approaches 0) as shown in Fig. 4(b).

For the same reason as stated above, the reflection and transmission coefficients at the control location can be expressed as

$$t_3=1+\frac{\overline{H}\mathrm{i}}{4-(1+\mathrm{i})\overline{H}},\quad r_3=\frac{\overline{H}\mathrm{i}}{4-(1+\mathrm{i})\overline{H}} \tag{30}$$

where t_3 and t_4 are the transmission coefficients, r_3 and r_4 the reflection coefficients.

2.3 Controller design

The optimal controller is noncausal[5-6]. Hence, a real-time implementation must be some approximations to this ideal. PD feedback control is implemented, with the controller tuned so that it is equal to the optimal controller at some specific frequencies ω_d. The controller then has the frequency response

$$H_w(\omega)=c_1+c_2(\mathrm{i}\omega) \tag{31}$$

where $c_1=\omega_d g$ and $c_2=g$.

If the force is applied at a point $x_i=x_w$ $(i=1,2)$, then the wave-control force is $f_w=(w,x_i,t)\delta(x_i t x_w)$. For tuned PD control, substituting Eq. (31) to Eq. (20), using Laplace transform, this becomes

$$f_w(x_i,t)=-[c_1 w(x_i,t)+c_2\dot{w}(x_i,t)]\delta(x_i-x_w) \tag{32}$$

For collocated wave control, and with the control force approximated by Eq. (32), the equations of motion can thus be written in matrix form as

$$\widetilde{\boldsymbol{M}}\ddot{\boldsymbol{z}}+\widetilde{\boldsymbol{C}}\dot{\boldsymbol{z}}+\widetilde{\boldsymbol{K}}\boldsymbol{z}=\boldsymbol{B}^{\mathrm{T}}\boldsymbol{F}(t) \tag{33}$$

3 NUMERICAL EXAMPLES

In this section, some numerical results are presented. In what follows, several dimensionless parameters are: $L=1$, the first natural frequency of the first beam $\omega_1=1$, the thickness ratio of two beams $\sigma=0.90$, 0.21 and 0.05, and the corresponding non-dimensional natural frequencies $\overline{\omega}_i (i=1,2,\cdots,9)$ are given in Tables 1—3.

Table 1 First nine nondimensional natural frequencies of system (σ=0.90)

Mode number	1	2	3	4	5	6	7	8	9
Frequency	5.79	11.54	21.62	27.37	40.45	48.39	65.29	75.59	96.51

Table 2 First nine nondimensional natural frequencies of system (σ=0.21)

Mode number	1	2	3	4	5	6	7	8	9
Frequency	1.88	4.45	8.05	11.63	15.53	22.04	32.38	52.82	78.68

Table 3 First nine nondimensional natural frequencies of system (σ=0.05)

Mode number	1	2	3	4	5	6	7	8	9
Frequency	0.58	1.15	2.07	3.38	5.08	12.08	33.86	57.70	82.42

A disturbance force is applied at $x_1=0.10L$. Simulation results are shown in Figs. 5—14. In Figs. 6, 14, the wave-control force is applied at $x_2=L$ when $\sigma=0.90$. In Fig. 8, the wave-control force is applied at $x_1=0.15L$ when $\sigma=0.05$. In Fig. 10, the wave-control force is applied at $x_2=L$ when $\sigma=0.21$ (reflected energy at the beam junction is almost equal to transmitted energy of the beam junction). In Fig. 11, the wave-control force is applied at $x_1=0.15L$. In Fig. 12, two wave controllers are applied at $x_1=0.15L$ and $x_2=L$. Numerical results show the response at $x_2=0.75L$ per unit disturbance force. In Figs. 5—12, the value of ordinate is prescribed as common logarithm of the actual deflection.

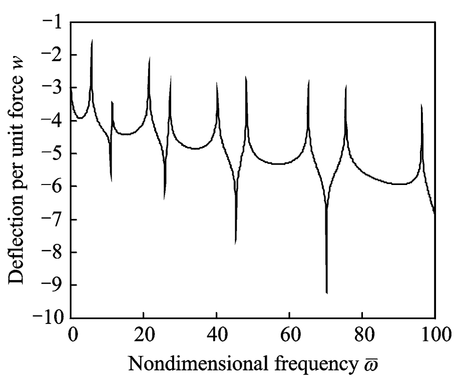

Fig. 5 Frequency response before wave control ($\sigma=0.90$)

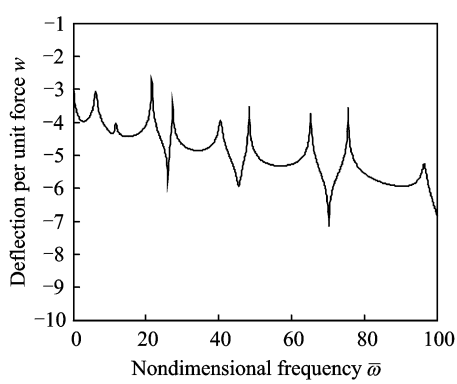

Fig. 6 Frequency response after wave control ($\sigma=0.90$, $x_2=L$)

The positions of these points are chosen so as to avoid the nodes of the modes. The controlled and uncontrolled frequency responses are compared. In the approximation that tuned PD control, the controller is tuned to be optimal at $\omega_d=10$.

Figs. 5, 6 show that the frequency responses before and after wave control when $\sigma=0.90$. The power is mostly transmitted at the beam junction when σ is close to 1, so wave controller is applied at the second beam for good performance. Without control, sharp resonances can be observed. While after wave control, controllers add damping to the structure. Energy of structure is absorbed. Sharp resonances are weakened.

Figs. 7, 8 show that the frequency responses before and after wave control when $\sigma=0.05$. The power is mostly reflected at the beam junction when σ approaches 0. Therefore, wave control is applied at the first beam. In Figs. 6, 8, relatively poor performance can be seen. The degradation of the performance is due to the fact that the point of application of the wave controller lies to the nodes of the modes. Such effects depend on the specific form and location of the wave controller, the conclusion is same as Refs. [5, 12]. They can be minimized by the suitable application of two or more wave controllers.

Figs. 9—12 show that the frequency respon-

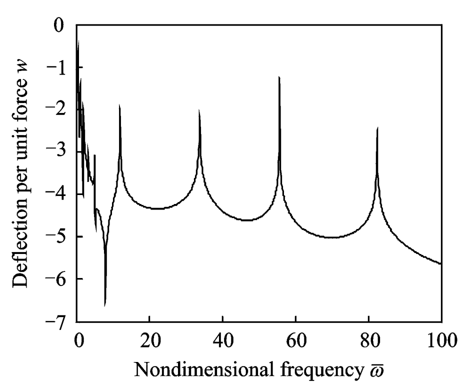

Fig. 7 Frequency response before wave control ($\sigma=0.05$)

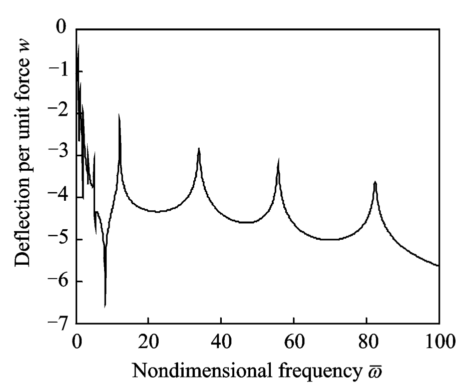

Fig. 8 Frequency response after wave control ($\sigma=0.05$, $x_1=0.15L$)

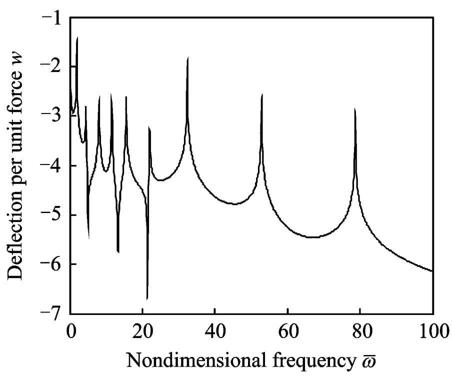

Fig. 9 Frequency response before wave control ($\sigma=0.21$)

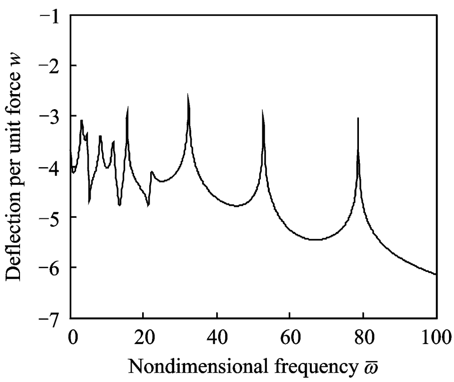

Fig. 10 Frequency response after wave control ($\sigma=0.21$, $x_2=L$)

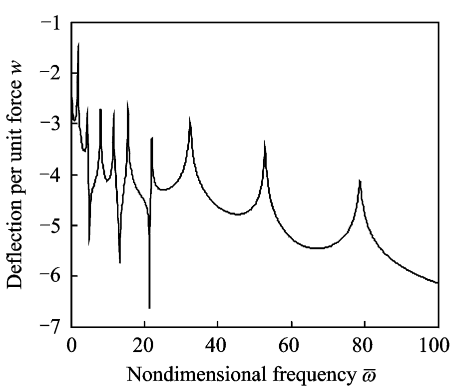

Fig. 11 Frequency response after wave control ($\sigma=0.21$, $x_1=0.15L$)

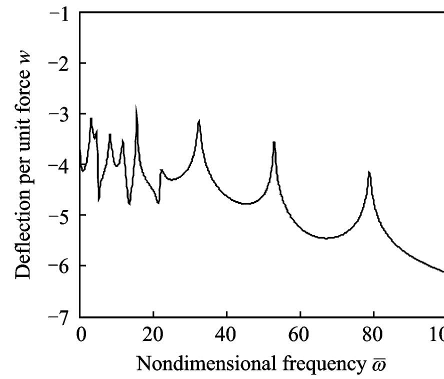

Fig. 12 Frequency response after wave control ($\sigma=0.21$, $x_1=0.15L$, $x_2=L$)

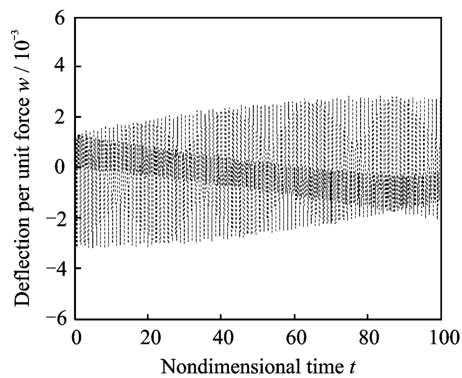

Fig. 13 Time response before wave control ($\sigma=0.90$)

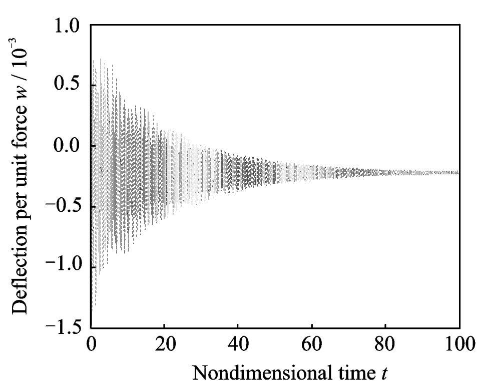

Fig. 14 Time response after wave control ($\sigma=0.90$)

ses before and after wave control when $\sigma=0.21$. Fig. 10 shows wave controller absorbs vibrational energy, especially at lower frequencies. Fig. 11 shows wave controller absorbs vibrational energy, especially at higher frequencies. In Figs. 10, 11, relatively poor performance can be seen when wave controller is only applied at the downstream of the beam junction or upstream of the beam junction, whereas Fig. 12 gives better performance. In fact, reflected energy at the beam junction is almost equal to transmitted energy at the beam junction when σ approaches 0.21, so wave controllers are ought to be applied at not only the first beam but also the second beam for better performance. One controller absorbs reflected energy, and the other absorbs transmitted energy. Figs. 13, 14 show that the time responses before and after wave control when $\sigma=0.90$.

4 CONCLUSION

This paper presents the theoretical analysis and numerical results of wave control of two-beam structures. Wave control is used to control the wave motion of the structures. The incident propagating wave is reflected and transmitted at beam junction, and wave reflection and transmission coefficients at beam junction are also be decided by the thickness ratio of two coupled beams. The power is mostly transmitted at the beam junction when the thickness ratio σ is close to 1. When σ is close to 0, the power is mostly reflected at the beam junction. Therefore wave control is used somewhere downstream to absorb energy associated with the transmitted propagating wave of the beam junction when σ is close to 1. When σ is close to 0, wave control is used somewhere upstream to absorb energy associated with the transmitted propagating wave of the beam junction. In other circumstances, there is not only reflected energy at the beam junction but also transmitted energy. Now, better performance can be achieved by applying wave controllers to two sides of beam junction. One controller absorbs reflected energy, and the other absorbs transmitted energy.

Control gain is designed in frequency domain. PD control is adopted. In the time domain, this corresponds to a tuned spring-damper combination. The results show that the wave control is efficient for two coupled beams. Similarly, the wave controller is designed for two coupled plates lying in the x-y plane and its efficiency is proved.

References:

[1] Ma Xingrui, Gou Xingyu, Li Tieshou, et al. Development generalization of spacecraft dynamics [J]. Journal of Astronautics, 2000,21(3):1-5. (in Chinese)

[2] Wang Liang, Chen Huaihai, He xudong, et al. Active vibration control of axially moving cantilever beam by magnetic force[J]. Journal of Nanjing University of Aeronautics & Astronautics, 2010,42(5):568-573. (in Chinese)

[3] Miller D, Hall S, Flotow A von. Optimal control of power flow at structural junctions [J]. Journal of Sound and Vibration, 1990,140 (3):475-497.

[4] Jha R, Bailey A, Ahmadi G. Combined active and passive control of space structure vibrations during launch [C]//44th AIAA/ASME/AHS Structures, Structural Dynamics, and Materials Conference. Norfolk, Virginia, USA: AIAA, 2003.

[5] Mei C, Mace B R, Jones R W. Hybrid wave/mode active vibration control[J]. Journal of Sound and Vibration, 2001,247(5):765-784.

[6] Chen T, Hu C, Huang W H. Vibration control of cantilevered Mindlin-type plates[J]. Journal of Sound and Vibration, 2009,320(1/2):221-234.

[7] Gardonio P, Elliott S J. Active control of waves on a one-dimensional structure with a scattering termination[J]. Journal of Sound and Vibration, 1996,192 (3):701-730.

[8] Brennan M J. Control of flexural waves on a beam using a tunable vibration neutralizer [J]. Journal of Sound and Vibration, 1998,222(3):389-407.

[9] Carvalho M O M, Zindeluk M. Active control of waves in a Timoshenko beam[J]. International Journal of Solids and Structures, 2001,38(10-13):1749-1764.

[10] Halkyard C R, Mace B R. Feedforward adaptive control of flexural vibration in a beam using wave amplitudes[J]. Journal of Sound and Vibration, 2002,254 (1):117-141.

[11] EL-Khatib H M, Mace B R, Brennan M J. Suppression of bending waves in a beam using a tuned vibration absorber [J]. Journal of Sound and Vibration, 2005,288(4/5):1157-1175.

[12] Hu Chao, Chen Tao, Huang Wenhu. Active vibration control of Timoshenko beam based on hybrid wave/mode method[J]. Acta Aeronautica et Astronautica Sinica, 2007,28(2):301-308. (in Chinese)

[13] Mace B R. Wave reflection and transmission in beams[J]. Journal of Sound and Vibration, 1984,97 (2):237-246.

[14] Mead D J. Waves and modes in finite beams: Application of the phase-closure principle [J]. Journal of Sound and Vibration, 1994,71(5):695-702.

[15] Svensson J L, Andersson P B U, Kropp W. On the design of structure junctions for the purpose of hybrid passive-active vibration control[J]. Journal of Sound and Vibration, 2010,329(9):1274-1288.

[16] Meirovitch L. Dynamics and control of structures [M]. New York: Wiley, 1990.

(Executive editor: Zhang Huangqun)